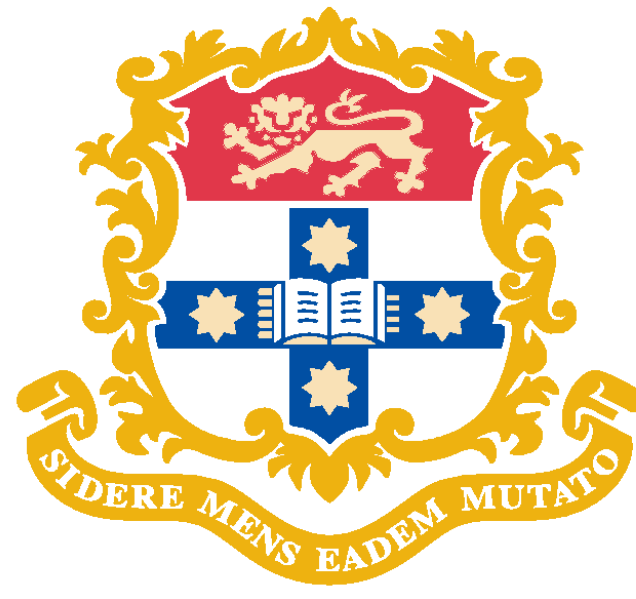


Linking Geological Observations to Forward Models of Dynamic Topography in the South West Pacific since the Mesozoic



Lydia J. DiCaprio¹, Michael Gurnis², R. Dietmar Müller¹

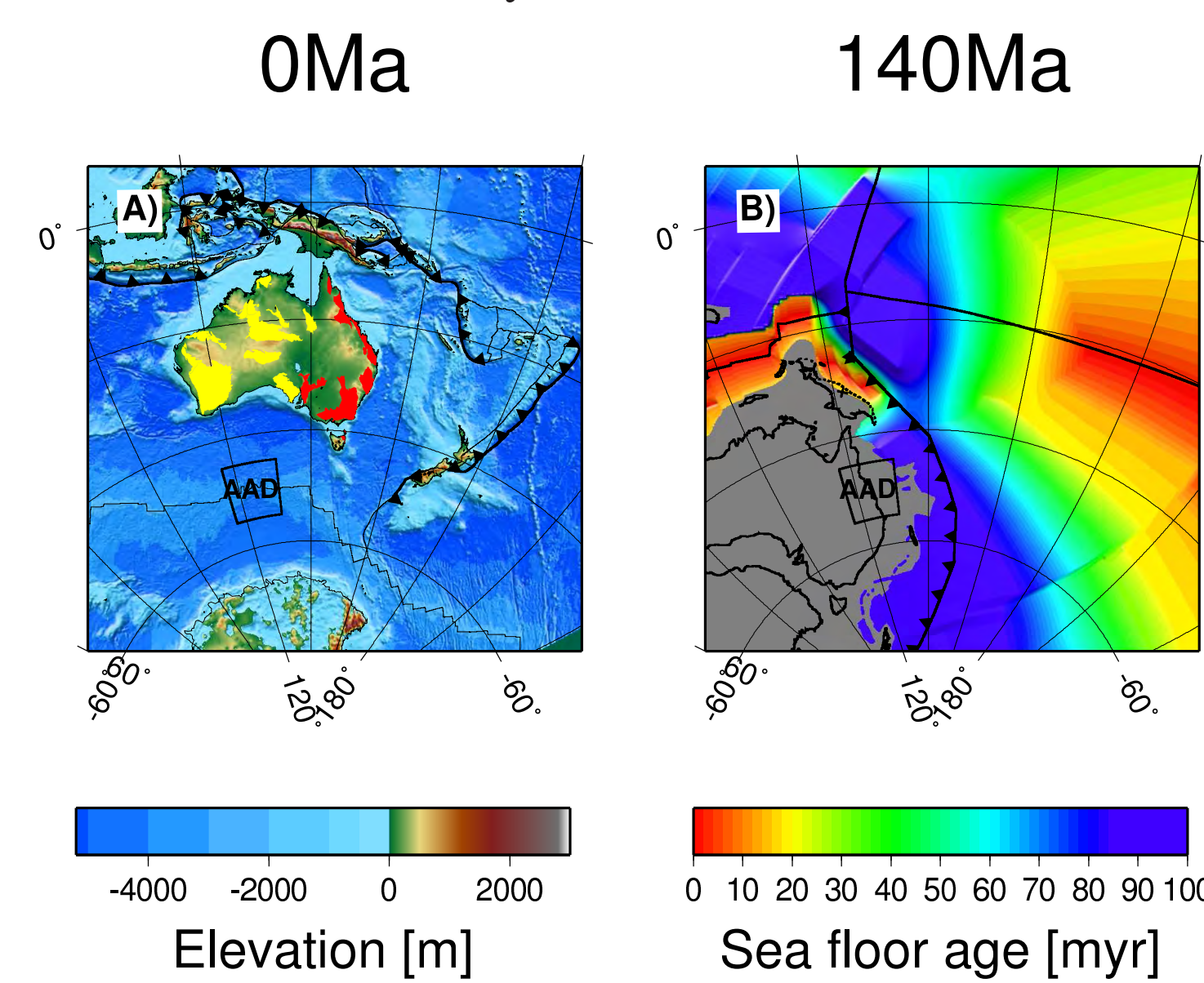
1: School of Geosciences, University of Sydney 2: Seismological Laboratory, California Institute of Technology contact: lydia@gps.caltech.edu



Introduction

Marine advance and retreat into continental interiors is highly susceptible to evolving buoyancy in the mantle if the topography produced by convective process is of a similar magnitude to global sea level fluctuations. Here we explore the evidence for mantle convective processes producing topography on the Australian continent since the Late Cretaceous. We describe the evolving trend of the anomalous topography and its relationship to subduction in South East Asia. Next we test the relationship between these long wavelength patterns and the subduction history around the Australian continent.

Figure 1. The topography of the Australian continent with present day plate boundaries. Australia is a stable continent and has experienced few major tectonically driven topographic changes since the Late Cretaceous. A) Australia is largely composed of old stable cratonic fragments (yellow polygons) and fold belts which were active since the Palaeozoic (red). The stability of its cratonic blocks and the relative tectonic quiescence since the Cretaceous makes Australia a prime candidate to study the potential magnitude of convective processes on surface topography. B) 140 million years ago Australia was located close to long-lived westward dipping subduction located on the eastern margin of Gondwanaland. Here we propose that subduction at the subduction systems around Australia have caused inundation into the continent which is preserved in the Australian geological record. NB: If fixed relative to the mantle the Australian Antarctic Discordance (AAD) is now located on the north eastern margin of Australia.



Geological Observations from the Australian continent

Compared to the global sea level curve, the inundation history of the Australian continent does not behave as expected. The geologic record preserves the distribution of marine sedimentation recording the extent of marine incursion into the Continent. This record shows that Australia became progressively inundated throughout the Cenozoic despite a fall in global sea level (fig. 2). Since Australia was relatively isolated from tectonic processes this pattern of inundation indicated that there is a component of anomalous topography.

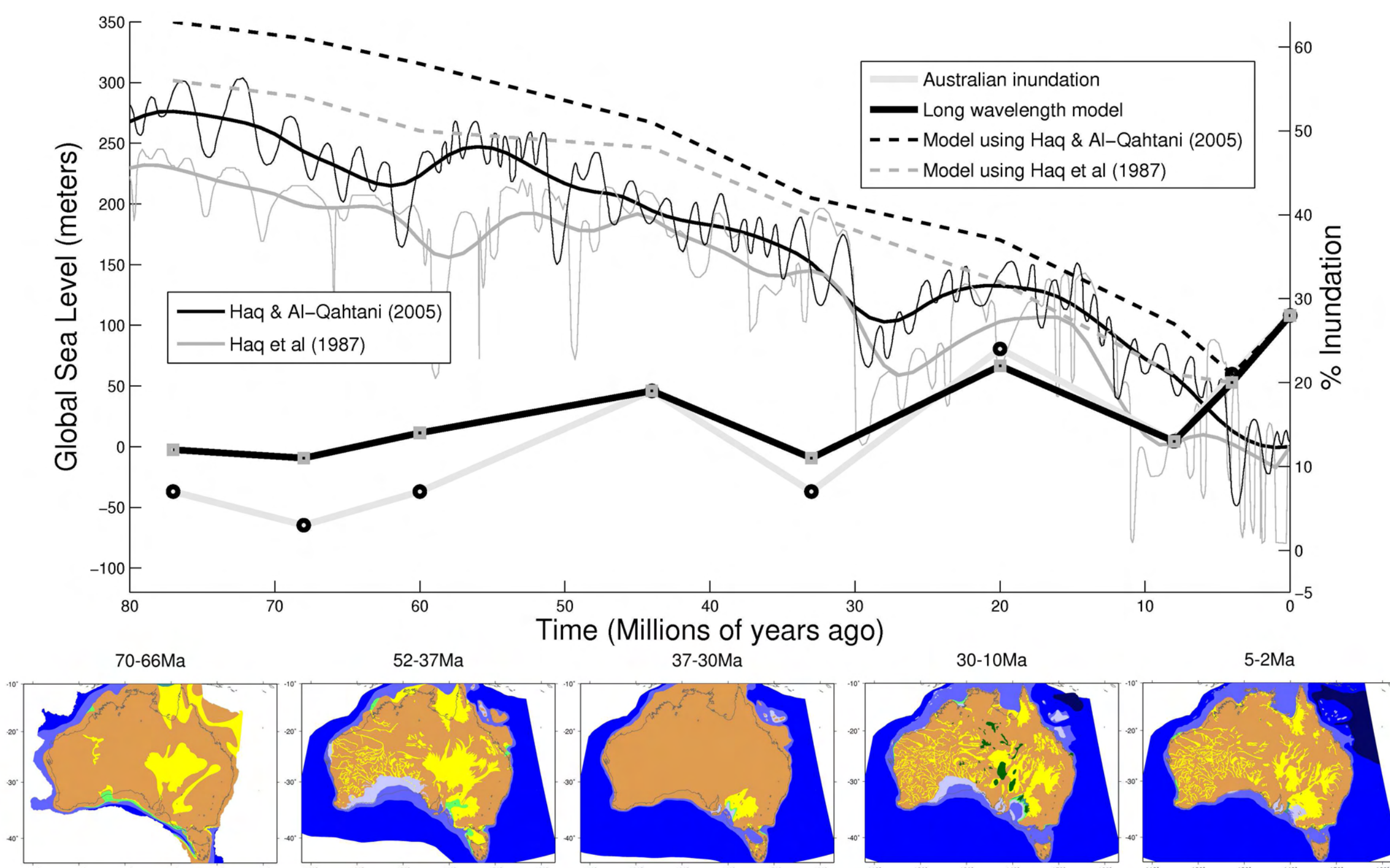


Figure 2. Global sea level and the pattern of marine inundation on the Australian continent since the Late Cretaceous are inconsistent. Plotted is the inundation history of Australia since the Late Cretaceous, modeled inundation and global sea level. We create modeled inundation by removing the effect of sediment loading and then we inundate the continent with global sea level (broken lines). Time is the midpoint of paleogeographic mapping intervals (Langford et al., 1995). A selection of these paleogeographic maps are shown below the graph and show the increase of marine incursion into the Australian continent since the Late Cretaceous.

Method for extracting the underlying dynamic signal

We quantify the inconsistency between expected and observed patterns of inundation.

We apply published global sea level curves (Haq and Al-Qahitani, 2005; Haq, et al., 1987) to modeled topography. Then we isolate the topography that is the result of convective processes by comparing the predicted pattern of inundation with an observed pattern of marine inundation. We remove topography which is thought to be influence by tectonic processes such as subsidence due to lithospheric stretching or mountain building from distal or proximal plate boundaries.

We quantify the anomalous vertical motion of the Australian continent in three steps:

- **Interpreted Inundation:** We use the paleo-shoreline from published paleogeographic maps (Langford et al., 1995). These maps are broken into intervals ranging in length from 3 to 19.6 Myr between 80 Ma and 1.6 M years ago and are constrained by 361 data points, primarily bore holes (fig. 3).
- **Predicted Topography:** We predict the pattern of inundation for each time interval by sequentially removing the effect of sediment loading from present day topography (etopo2 N.O.A.A. 2006) and changing the sea level according to a global sea level curve (Haq and Al-Qahitani, 2005; Haq, et al., 1987).
- **Modeled Topography:** The predicted topography is sampled along the interpreted paleo-shoreline. This represents the displacement required to reconcile the predicted pattern of inundation to the interpreted paleo-shoreline. A planar surface is calculated using least squares regression to minimize the difference between the predicted pattern of inundation and the interpreted position of the paleo-shoreline.

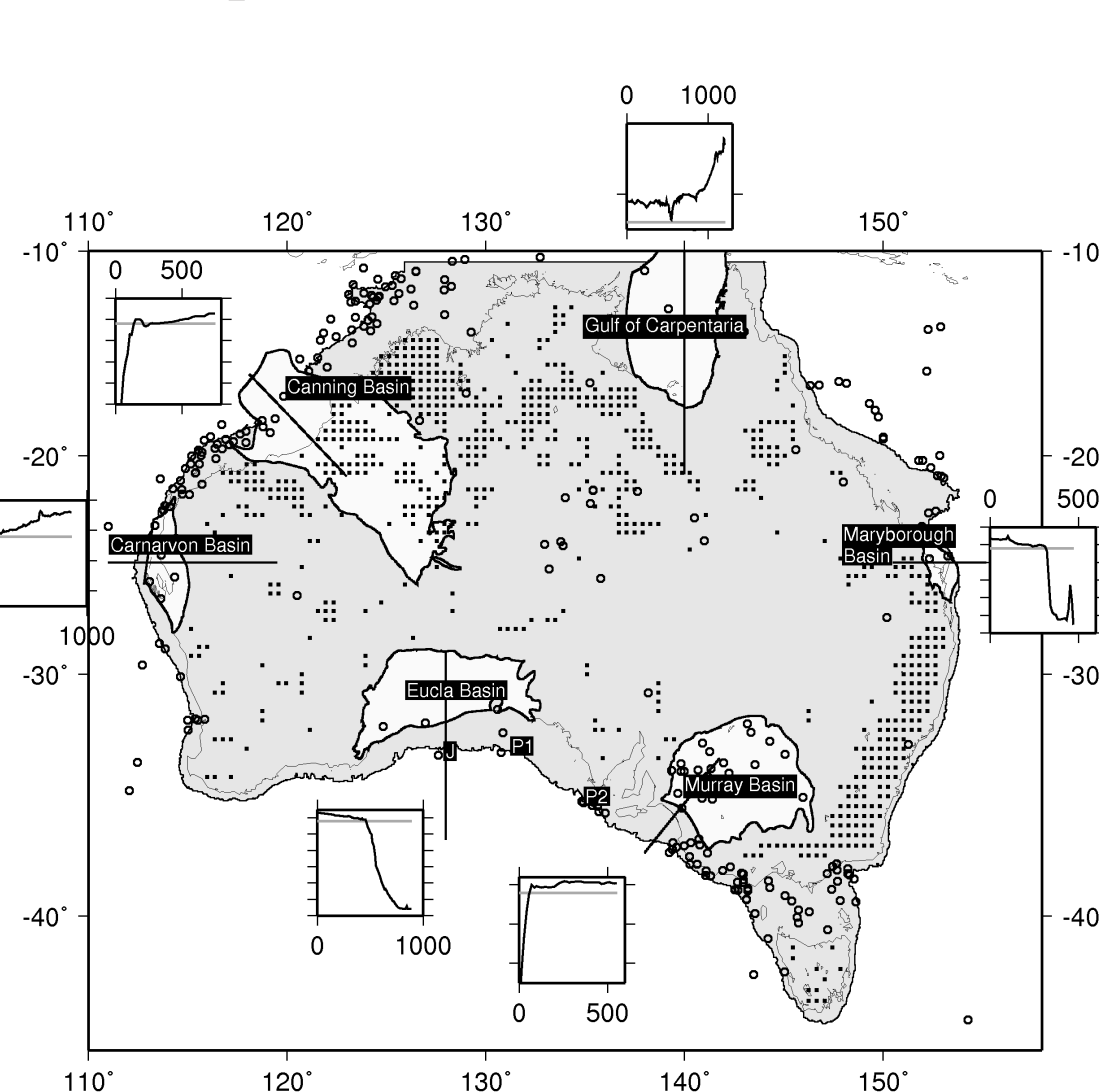
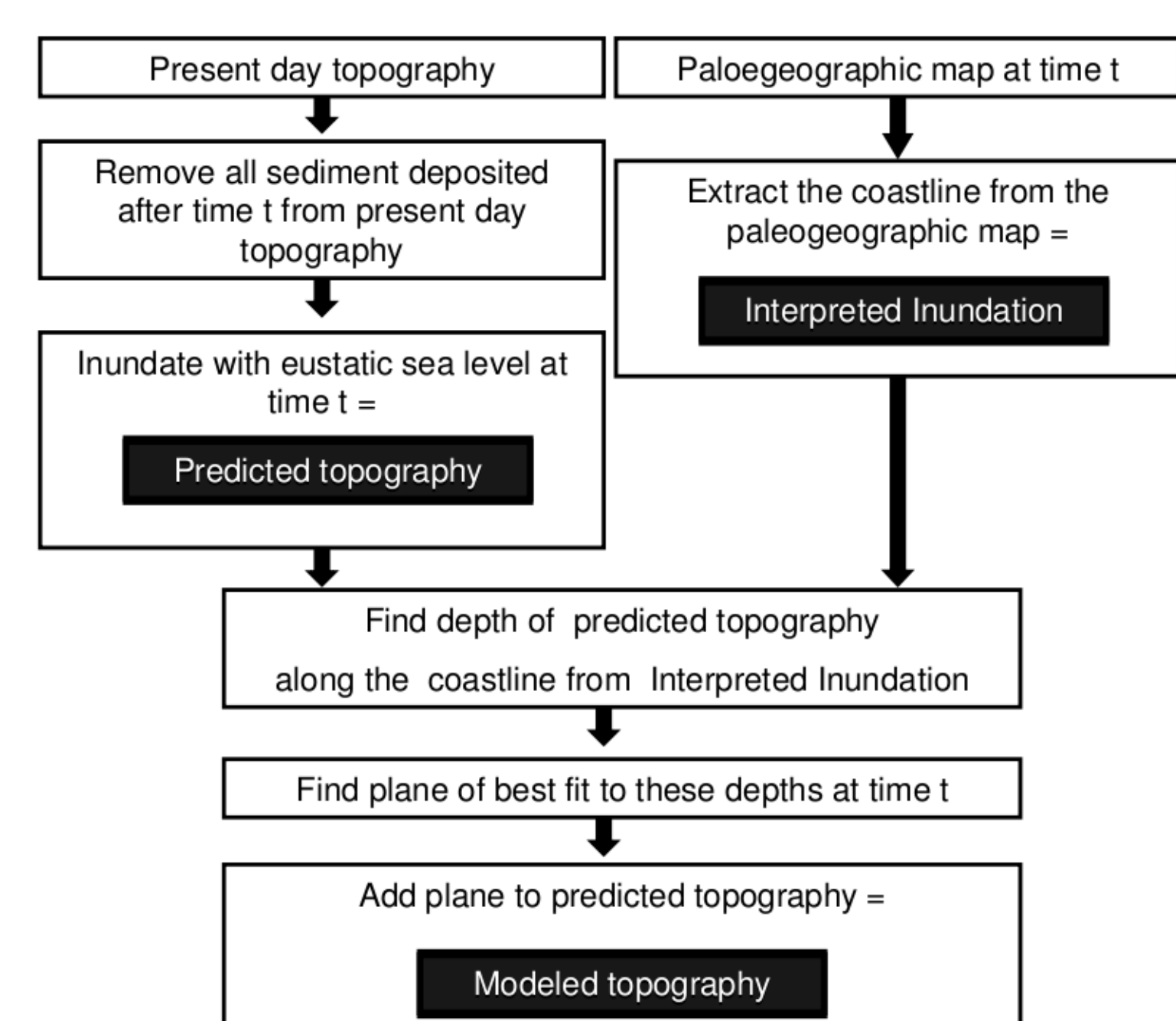


Figure 3. Left: Borehole data (circles) include those published with the paleogeographic maps Langford et al (1995), several from the Murray Basin adapted from Gallagher et al. (2007) and Brown et al. (2001). Erosional areas (squares) between 83 and 1 Ma are always set to 0. Six basins (shaded light grey) on the margins of the continent include a profile (black line) showing the shelf break (grey line) which is typically at 200 m depth below sea level. Vertical tick marks are at 1000 m intervals in each profile. The extent of the 200 m isobath is shaded grey.



Resulting Long Wavelength Anomalous Topography

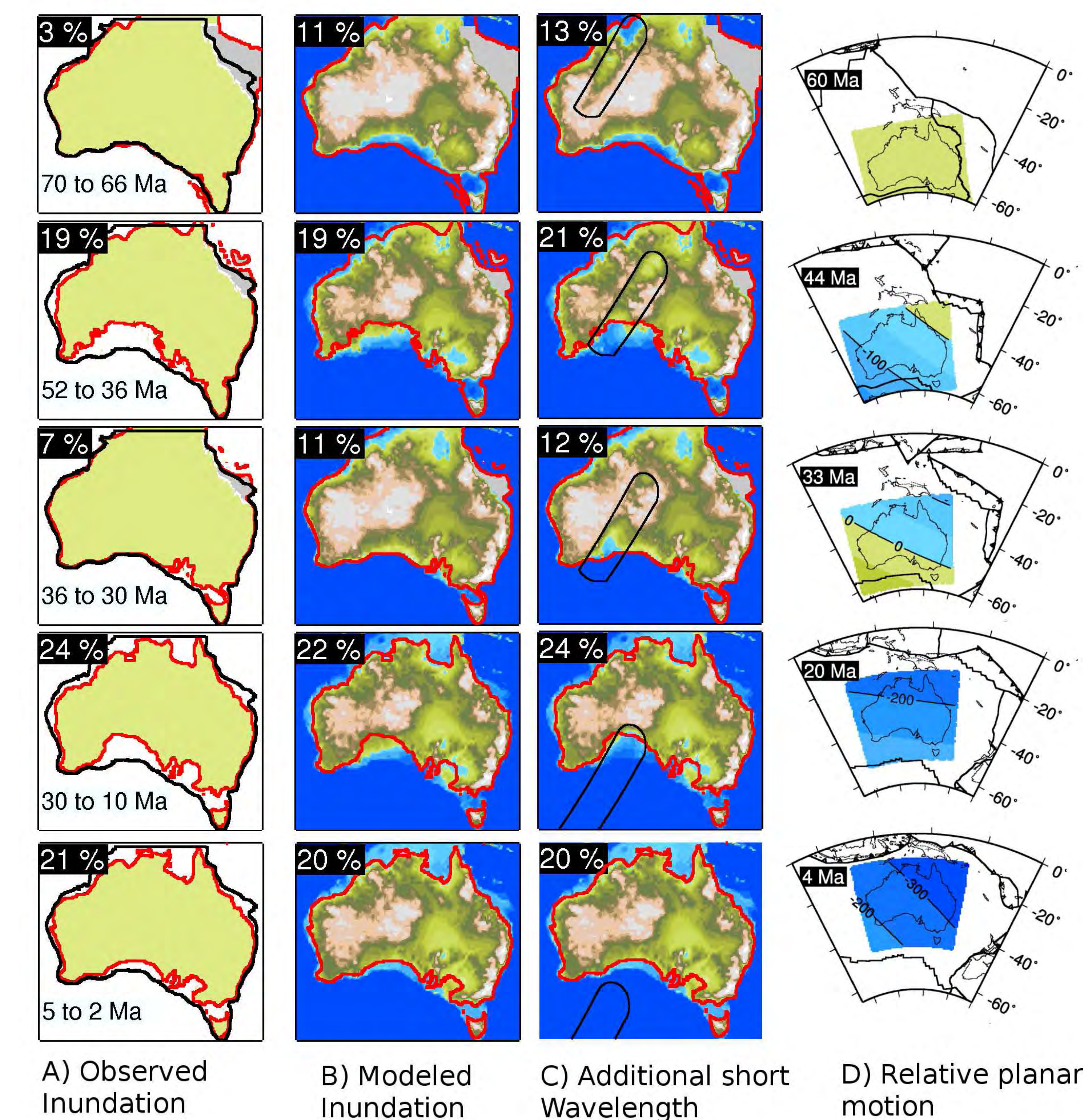


Figure 4. A) Observed inundation from paleogeographic maps (Langford et al., 1995) (shaded green and outlined in red) and the present day 200 m isobath is plotted in black. The percent of continental inundation in each map is shown in the top left corner. The area occupied by the northeastern marginal plateaus (shaded grey A, B, C) is removed from the calculation of the percent of continental inundation. B) Modeled inundation (with long wavelength adjustment). C) Modeled inundation with long wavelength dynamic topography and an additional 250 m deep short wavelength topography anomaly D) Relative motion of the long wavelength anomalous topography of Australia since 60 Ma. Shorter wavelength anomalous topography is added to the long wavelength and major plate boundaries were interpreted and reconstructed using the Gplates software.

Interpretation

Extracting the long wavelength component of this anomalous topography and plotting the continent according to its paleo-position demonstrates:

- **Relative motion since 60 Ma** As the spreading rate between Australia and Antarctica increased and after the initiation of subduction along the Greater Melanesian Arc (43 Ma, Hall, 2002) the northern margin of the Australian continent was progressively tilted downward by up to 300 meters toward the NE.
- **shorter wavelength component on the southern margin** The southern margin experienced long wavelength subsidence since the Oligocene (fig. 4). However, in order to account for the inundation of the southern margin of Australia (Eucla Basin) we need to apply a shorter wavelength component of topography. We use the occurrence of anomalous subsidence at boreholes to propose the shape of this anomaly. The paleo-position of this shorter wavelength anomalous topography is incident with the appearance of the closely spaced fracture zones on the South East Indian Ridge (20 Ma). The anomaly is also consistent with the descent of the slab beneath the Australian continent and the drawing up of this material at the Australian Antarctic Discordance (Gurnis et al., 1998). This anomaly provides the Tertiary link between subduction east of Australia, the inundation and uplift of the eastern interior basins during the Cretaceous and the formation of the Australian Antarctic Discordance (AAD).

Evidence from Bathymetry

The Australian Antarctic Discordance is the deepest segment of spreading ridge in the world. The bathymetric anomaly is roughly V shaped and extends from the continental margin of Australia to Antarctica.

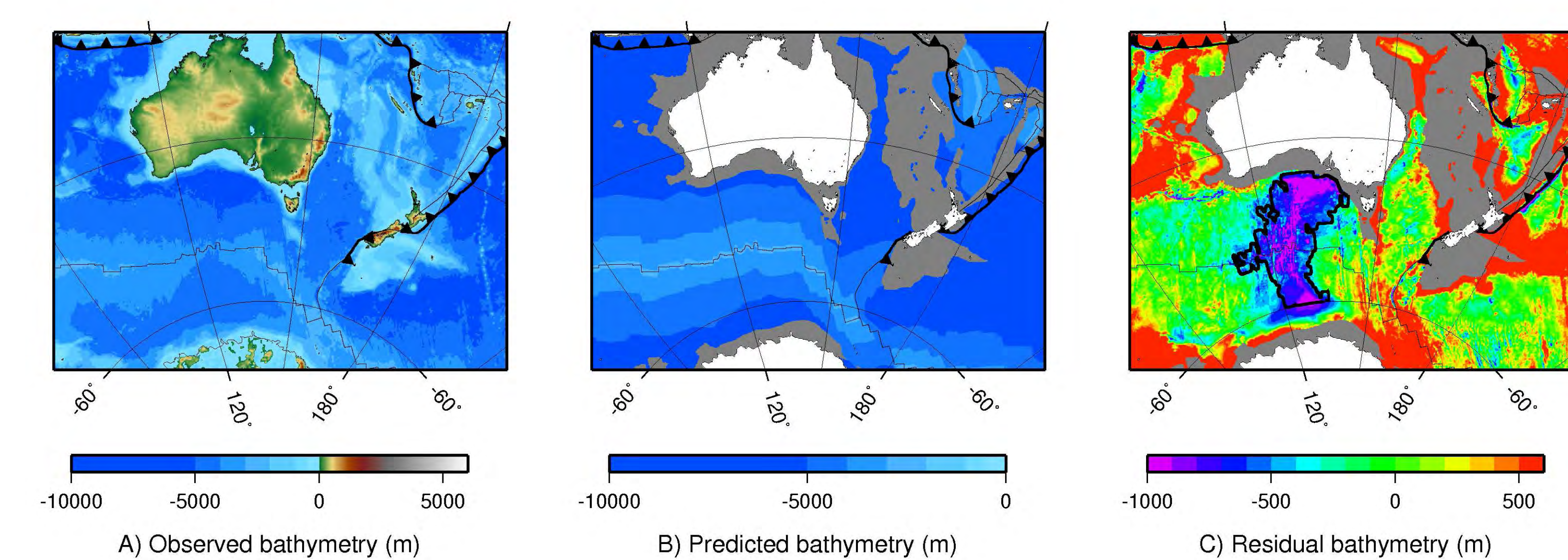


Figure 5. Residual topography calculated by taking the difference between observed bathymetry (sediment removed) and expected bathymetry from sea floor age.

Evidence from Tomography

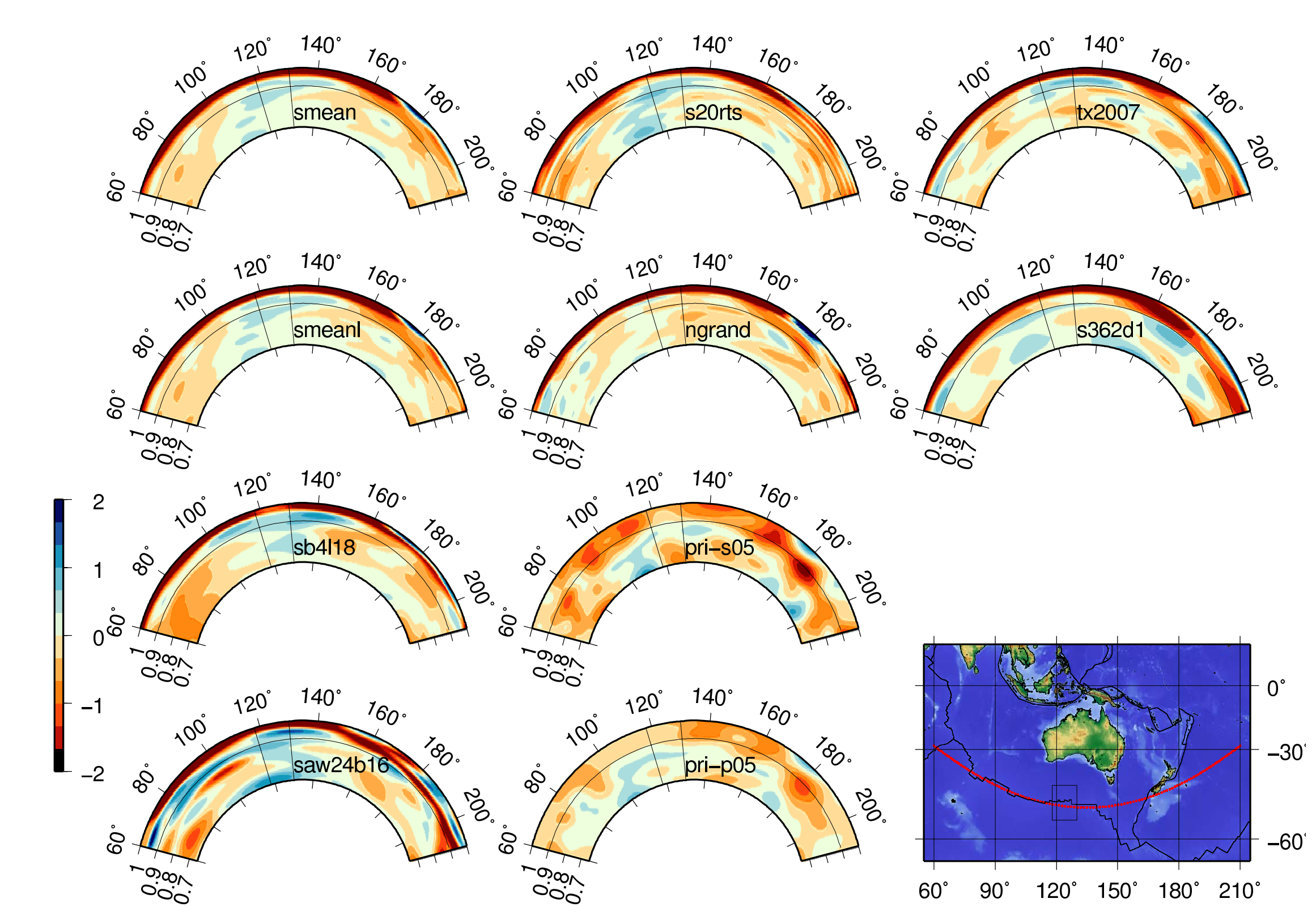


Figure 6. Sections through common tomography models at the AAD along the South East Indian Ridge. The box marks the location of the AAD. We can see that in most of the models a high velocity anomaly exists in the approximate location of the AAD. Models are: smeans and smeant with finer vertical sampling (Becker and Boschi 2002), sb4116 (Scripps), saw24b16 (Berkeley), s20rts (Ritsema et al.), ngrand (Grand), pri-s05 pri-p05 (Princeton Montelli et al., 2006), b2007 (Simmons et al. 2007), s362d1 (Harvard).

Geodynamic Models

What is the origin of the short wavelength anomaly that caused the additional subsidence beneath the southern margin of Australia? What is the origin of the material now sitting beneath the AAD? With geodynamic models can we account for the northward tilting of the Australian continent since the Eocene and can we tie these anomalous geological observations on and offshore directly to subduction processes?

Here we present 3D forward models of mantle convection. These models incorporate plate motion as a surface velocity boundary condition, evolving sea floor age (Müller et al., 2005) as a surface thermal layer, compositionally dependant viscosity to incorporate strong cratonic roots and passive tracers which map the evolution of geochemical provinces within the mantle. We use the finite element package CitcomS (Tan et al., 2006) available from the Computational Infrastructure for Geodynamics (CIG) <http://geodynamics.org>. We use a temperature and depth dependent viscosity governed by the rheology law $\eta = \eta_0 e^{T + \eta_1 \frac{T}{1 + \eta_2}}$

Lithosphere 0 – 125 km	$\eta = 2e^{21}$ Pas	non-d	$\eta_E = 7$
Asthenosphere 125 – 410 km	$\eta = 1e^{20}$ Pas	non-d	$\eta_E = 7$
Transition zone 410 – 670 km	$\eta = 4e^{21}$ Pas	non-d	$\eta_E = 7$
Lower mantle 670 – 2800 km	$\eta = 3e^{22}$ Pas	non d	$\eta_E = 7$

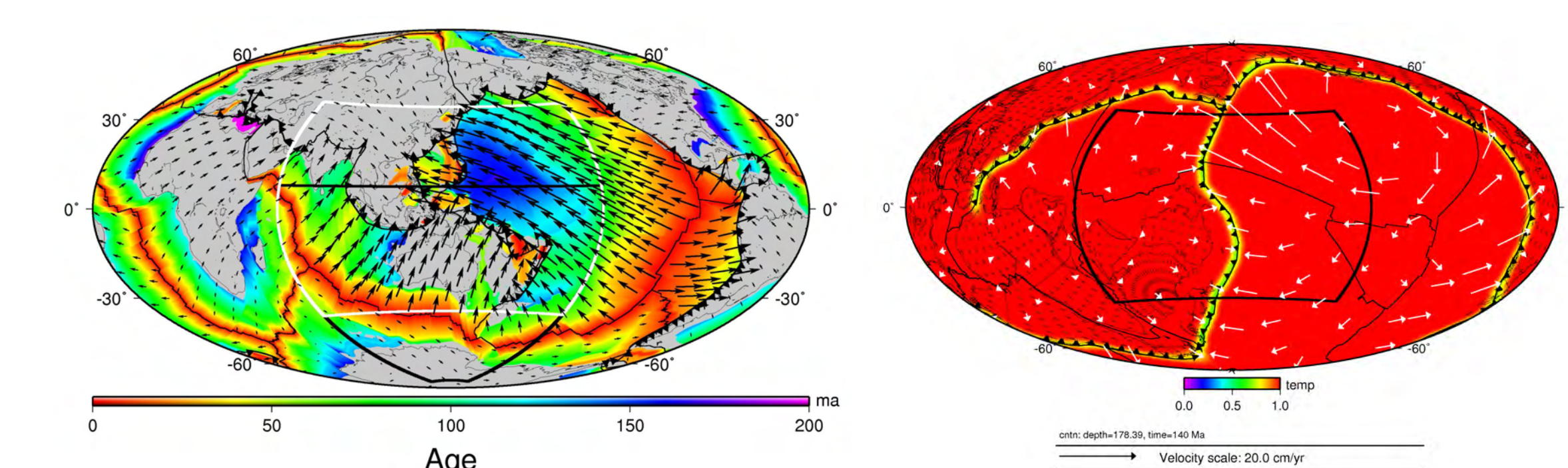


Figure 7. Left: Global plate age and plate velocities at 0 Ma based on an absolute moving hot-spot reference frame (Oneill et al., 2005). Plate velocities generated using gplates (available from <http://gplates.org>). The Australian region at the pole (black box) is rotated to the equator (white box). Right: The global temperature initial condition at depth.

Since the evolution of the slab is influenced by whole mantle flow we use nested solver coupling to accurately and efficiently solve this multi-scale geophysical problem (Tan, 2004) whereby two CitcomS solvers are coupled to investigate the interaction of the subducted slab beneath the Australian plate with global mantle flow at low resolution.

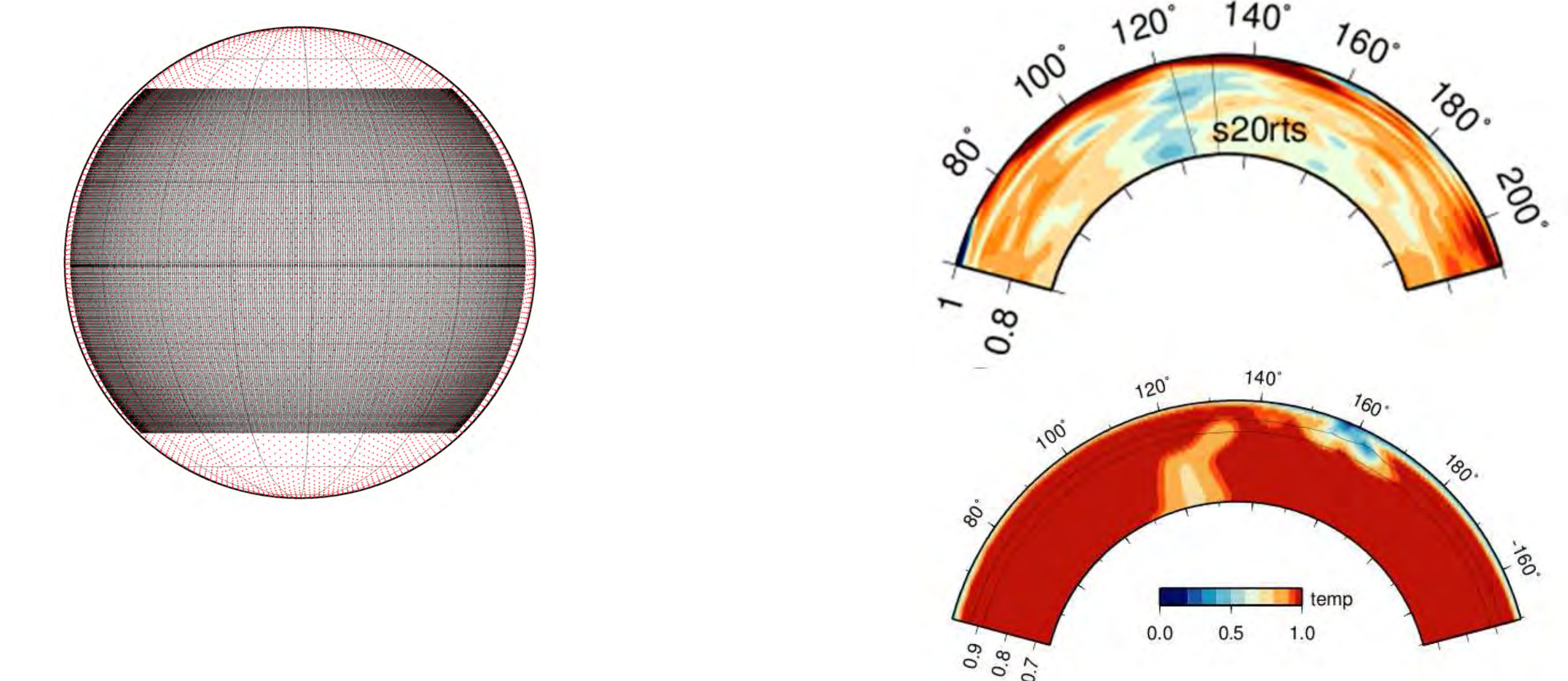


Figure 8. The embedded mesh (black points) and the containing mesh (red points).

Figure 9. Comparing the output of our geodynamic model to S20rts tomography.

Modeled Dynamic Topography

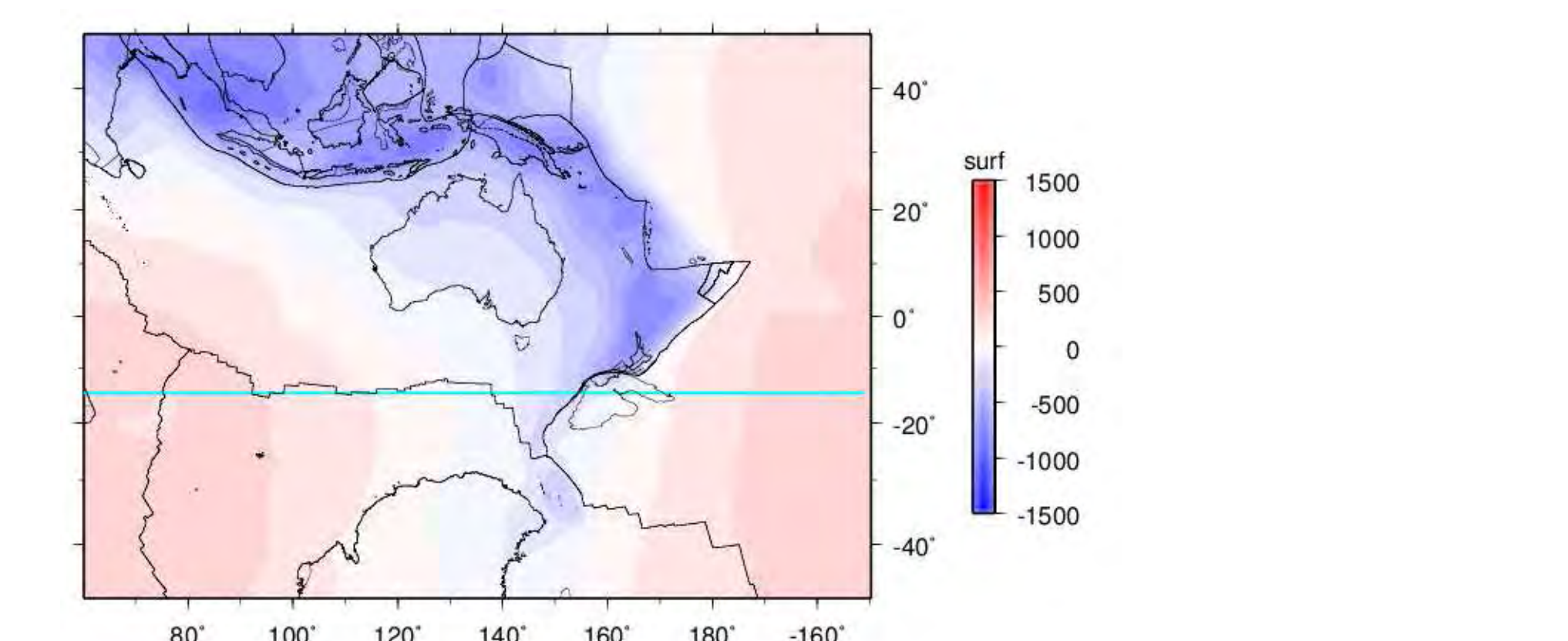


Figure 10: Dynamic topography at 0 Ma.

Our models show that as Australia moves northward toward the subduction realm in South East Asia a long wavelength tilt is formed across the continent. This north downward tilting is similar in magnitude and orientation to the tilting we observed from our paleo-shoreline analysis. Although the slab appears to correlate well with a fast velocity anomaly beneath the AAD we are not able to match the topographic signature at the AAD. Further testing with a high viscosity mantle wedge may allow the viscous stress from the sinking slab to transfer to the surface.